

## Optical search limit and preferred position angles of galaxies in 35 clusters

B. Aryal,<sup>1,2\*</sup> R. K. Bachchan<sup>2</sup> and W. Saurer<sup>1</sup>

<sup>1</sup>*Institute of Astro- and Particle Physics, Innsbruck University, Technikerstrasse 25  
A-6020 Innsbruck, Austria*

<sup>2</sup>*Central Department of Physics, Tribhuvan University, Kirtipur, Kathmandu, Nepal*

Received 2010 October 23; accepted 2010 November 22

**Abstract.** We worked on POSSII and ESO films and measured the diameters and position angles of 6244 galaxies in 35 clusters using a 25-fold magnification microscope. The optical search limit has been estimated for these clusters. The position angle distributions of galaxies in the clusters have been studied. For this, chi-square, auto-correlation and the Fourier tests have been carried out. A dependence has been noticed between the optical search limit and the mean radial velocity of the cluster. The preferred position angle distribution of galaxies in the cluster has been found to be independent of the mean radial velocity of the cluster. Possible explanations of the result are discussed.

*Keywords :* catalogues – surveys – galaxies: clusters: general – galaxies: distances and redshifts – galaxies: evolution – galaxies: statistics

### 1. Introduction

Galaxy clusters are generally not in dynamical equilibrium (Peebles 1988), as there haven't been enough crossing times since their formation. They are useful probes of the mass distribution as they subtend large angles in the sky, and thus have many background objects which could be lensed. Their mass distributions and lensing potentials are however more complicated than those of a single galaxy (Barkanan & Loeb 2003). Argyres et al. (1986) reported that the population of galaxies are systematically higher in the direction of the major axes of the brightest galaxy in rich clusters. Adams, Strom & Strom (1980) studied seven Rood-Sastry L-type Abell clusters

---

\*e-mail:binil.aryal@uibk.ac.at

and found a weak tendency of the galaxy position angle (PA) to concentrate along the cluster PA and perpendicular to it. MacGillivray & Dodd (1979a, 1979b, 1985) investigated several groups and clusters and found a weak tendency of galaxies to be aligned with, or perpendicular to, their radius vectors to the cluster or group centre. Godwin *et al.* (1983) published machine measurements of 6727 galaxies in the Coma region. Djorgovski (1983) analysed their data and observed prominent alignment effects. He found that galaxies tend to align in the east-west direction with a high degree of significance. Strom & Strom (1978) studied the Perseus-Pisces Supercluster and noticed a distinct preference of the ellipticals to align with the main cluster chain. Gregory *et al.* (1981) noticed alignments and perpendicularity on a larger scale in the Perseus-Pisces Supercluster. Thompson (1976) noticed a tendency for galaxies in Coma to point towards the cluster centre.

Aryal & Saurer (2004, 2005, 2006) and Aryal, Paudel & Saurer (2007) noticed a systematic change in the galaxy alignments from early-type (Bautz-Morgan type I, hereafter BMI, Bautz & Morgan 1970) to late-type (BM III, irregular cluster) clusters while studying a database of 25 Abell clusters. Their result suggests that the spiral-rich (late-type) clusters (BM II-III and BM III) show a preferred alignment than those of elliptical-rich (early-type) clusters.

Gołowski *et al.* (2010) studied the spatial orientations of galaxies in the 247 optically selected rich Abell clusters and found that the values of statistics increase with the amount of galaxies members. They noticed a weak dependence between the preferred alignments and Bautz-Morgan type cluster morphology. In addition, they noticed that the velocity dispersion decreases with BM type at almost  $3\sigma$  level.

We present an analysis of the diameters and PAs of 6244 galaxies in 35 clusters and discuss their relations to the cluster mean radial velocity ( $RV$ ). In addition, assuming homogeneous distribution, the optical search limit is estimated for these clusters and their importance for further study discussed. The data and method of analysis are described in Sections 2 and 3. Finally, a discussion of the statistical analysis and conclusions are given in Sections 4 and 5 respectively.

## 2. Data

A cluster had to fulfill the following selection criteria in order to be selected: (1) the clusters had to have an Abell richness ( $R$ )  $\geq 1$ , (2) the  $RV$  of the cluster should be known, (3) the Bautz Morgan type morphology of the cluster should be given and, (4) clusters should be isolated. There were 107 clusters in the ACO (Abell, Corwin & Olowin 1989) catalogue fulfilling the selection criteria. We inspected all these clusters on the film copies (red sensitive ESO/POSS II) with the aid of a 25-fold magnification microscope, and selected 34 of them. The film-copies were illuminated from below. For the selected clusters, (i) the galaxies had to show a diffuse, non-stellar appearance; (ii) major diameter ( $a$ ) of member galaxies should be  $>10$  arcsec; (iii) the magnitude limit is chosen to be the tenth brightest magnitude of cluster galaxies ( $m_{10}$ ) and (iv) the films had to be available.

The search for galaxies was performed on the red sensitive ESO ( $\lambda_{eff} = 6400\text{\AA}$ ) and POSSII

films ( $\lambda_{eff} = 6400\text{\AA}$ ) having a limiting magnitude of  $m_{lim} = 20^m$ . The compilation of the catalogue consisted of six steps: (i) inspection of each film of interest by eye; (ii) re-examination of all objects detected in step 1; (iii) determination of the major ( $a$ ) and minor ( $b$ ) diameters of each galaxy candidate; (iv) measurement of PA of each galaxy candidate; (v) measurement of the position of each object; (vi) comparison of the final galaxy sample to known galaxies. A list

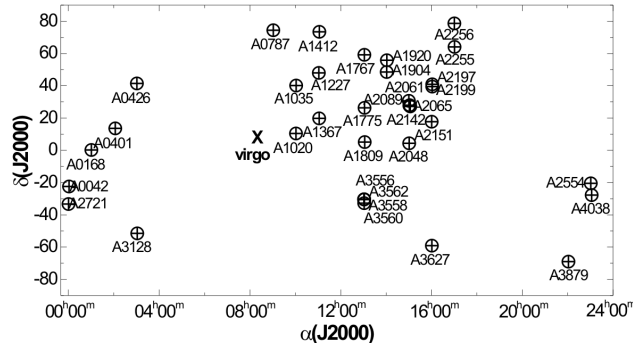


**Figure 1.** Distribution of 35 clusters in the equatorial coordinate system. The Virgo cluster (x) is also shown.

of all inspected film-copies is given in Table 1. The second step was the re-examination of the objects selected in step 1. Re-examination resulted in the rejection of more than 20% of the objects.

In order to measure diameters ( $a$ ,  $b$ ), a transparent scale with units of one tenth of a millimeter was placed on each object. The step size was 5 arcsec. Together with the determination of the diameters, the PAs were measured. A transparent glass with a hairy line was placed along the major diameter of the object. A protector of 15 cm radius was used to measure PA. The search for galaxies and the measurements of PAs and diameters ( $a$ ,  $b$ ) were carried out visually by one of the authors (to maintain homogeneity). The NASA/IPAC extragalactic database (NED) was used to check the compilation of galaxy samples in the catalogues. If available,  $RV$  and the morphology of the galaxy are noted.

A list of the investigated Abell clusters is given in Table 2. The data given in the second-sixth columns (cluster morphology,  $RV$ , the red magnitude of the tenth brightest cluster member ( $m_{10}$ ), distance class ( $D$ ) and richness ( $R$ )) in Table 2 are taken from the ACO catalogue.

The coordinates of the cluster centres given in the ACO catalogue were used to locate the clusters on the films. A circular survey area was defined using a radius  $r = 90''(1+z)^2/z$  (Thompson 1976). Here  $z$  represents the redshift of the cluster. All sky distribution of the clusters is shown in Fig. 1. The well studied Virgo cluster is added to our database. The database of the Virgo cluster is taken from Tully Nearby Galaxy catalog (Tully 1988), Virgo Cluster Galaxy catalog (Binggeli et al. 1985) and Uppsala General Catalog (Nilson 1973, 1974).

**Table 1.** The fields (third column) of ESO R and POSSII R (second column) searched for the clusters (first column). The right ascension ( $\alpha$ (J2000)) and declination ( $\delta$ (J2000)) of the cluster centre are listed in the last two columns.

Abell	print	field no.	$\alpha$ (J2000)	$\delta$ (J2000)
0042	ESO	473	00 <sup>h</sup> 28 <sup>m</sup> 36.5 <sup>s</sup>	-23°36'23"
0168	POSSII	825	01 <sup>h</sup> 15 <sup>m</sup> 09.8 <sup>s</sup>	+00°14'51"
0401	POSSII	616	02 <sup>h</sup> 58 <sup>m</sup> 56.9 <sup>s</sup>	+13°34'56"
0426	POSSII	301	03 <sup>h</sup> 18 <sup>m</sup> 36.4 <sup>s</sup>	+41°30'54"
0787	POSSII	037	09 <sup>h</sup> 28 <sup>m</sup> 33.7 <sup>s</sup>	+74°23'56"
1020	POSSII	710	10 <sup>h</sup> 27 <sup>m</sup> 50.7 <sup>s</sup>	+10°24'40"
1035	POSSII	317	10 <sup>h</sup> 32 <sup>m</sup> 07.3 <sup>s</sup>	+40°12'33"
1227	POSSII	216	11 <sup>h</sup> 31 <sup>m</sup> 34.6 <sup>s</sup>	+48°01'33"
1367	POSSII	572	11 <sup>h</sup> 44 <sup>m</sup> 29.5 <sup>s</sup>	+19°50'21"
1412	POSSII	039	11 <sup>h</sup> 55 <sup>m</sup> 45.2 <sup>s</sup>	+73°28'18"
1767	POSSII	132	13 <sup>h</sup> 36 <sup>m</sup> 00.3 <sup>s</sup>	+59°12'43"
1775	POSSII	509	13 <sup>h</sup> 41 <sup>m</sup> 55.6 <sup>s</sup>	+26°21'53"
1809	POSSII	793	13 <sup>h</sup> 53 <sup>m</sup> 18.9 <sup>s</sup>	+05°09'15"
1904	POSSII	222	14 <sup>h</sup> 22 <sup>m</sup> 07.9 <sup>s</sup>	+48°33'22"
1920	POSSII	175	14 <sup>h</sup> 27 <sup>m</sup> 16.9 <sup>s</sup>	+55°46'36"
2048	POSSII	797	15 <sup>h</sup> 15 <sup>m</sup> 17.8 <sup>s</sup>	+04°22'56"
2061	POSSII	449	15 <sup>h</sup> 02 <sup>m</sup> 15.3 <sup>s</sup>	+30°39'17"
2065	POSSII	449	15 <sup>h</sup> 22 <sup>m</sup> 42.6 <sup>s</sup>	+27°43'21"
2089	POSSII	450	15 <sup>h</sup> 32 <sup>m</sup> 41.3 <sup>s</sup>	+28°00'56"
2142	POSSII	515	15 <sup>h</sup> 58 <sup>m</sup> 16.1 <sup>s</sup>	+27°13'29"
2151	POSSII	584	16 <sup>h</sup> 05 <sup>m</sup> 15.0 <sup>s</sup>	+17°44'55"
2197	POSSII	331	16 <sup>h</sup> 28 <sup>m</sup> 10.4 <sup>s</sup>	+40°54'26"
2199	POSSII	331	16 <sup>h</sup> 28 <sup>m</sup> 37.0 <sup>s</sup>	+39°31'28"
2255	POSSII	101	17 <sup>h</sup> 12 <sup>m</sup> 31.0 <sup>s</sup>	+64°05'33"
2256	POSSII	023	17 <sup>h</sup> 03 <sup>m</sup> 43.5 <sup>s</sup>	+78°43'03"
2554	ESO	604	23 <sup>h</sup> 12 <sup>m</sup> 15.1 <sup>s</sup>	-21°33'56"
2721	ESO	349	00 <sup>h</sup> 06 <sup>m</sup> 14.5 <sup>s</sup>	-34°42'51"
3128	ESO	200	03 <sup>h</sup> 30 <sup>m</sup> 34.6 <sup>s</sup>	-52°33'12"
3556	ESO	444	13 <sup>h</sup> 24 <sup>m</sup> 06.2 <sup>s</sup>	-31°39'38"
3558	ESO	444	13 <sup>h</sup> 27 <sup>m</sup> 54.0 <sup>s</sup>	-31°29'00"
3560	ESO	383	13 <sup>h</sup> 31 <sup>m</sup> 50.5 <sup>s</sup>	-33°13'25"
3562	ESO	444	13 <sup>h</sup> 33 <sup>m</sup> 31.8 <sup>s</sup>	-31°40'23"
3627	ESO	137	16 <sup>h</sup> 15 <sup>m</sup> 32.8 <sup>s</sup>	-60°54'30"
3879	ESO	076	22 <sup>h</sup> 27 <sup>m</sup> 49.7 <sup>s</sup>	-69°01'41"

**Table 2.** Data of our sample. The first two columns list the Abell number and morphology (Bautz & Morgan 1970) of the cluster. The third and fourth columns give mean  $RV$  (in  $\text{km s}^{-1}$ ) and  $m_{10}$  of the cluster. The next two columns give the distance ( $D$ ) and richness class ( $R$ ) of the cluster. These values are taken from the ACO (Abell et al. 1989) catalogue. The last two columns give the total number of galaxies ( $N_T$ ) investigated (by the authors) in the cluster region and the galaxies with known PA ( $N$ ), respectively.

Abell	BM	$RV$	$m_{10}$	$D$	$R$	$N_T$	$N$
0042	I	32 587	17.1	5	3	165	130
0401	I	22 424	15.6	3	2	211	165
1775	I	20 866	15.7	4	2	135	122
2199	I	9 156	13.9	1	2	117	96
3556	I	14 360	16.4	4	2	163	146
3558	I	14 390	15.1	3	4	395	348
3560	I	14 660	15.1	3	3	159	138
3562	I	16 632	15.5	3	2	278	254
3627	I	4 881	14.2	1	1	65	59
3128	I-II	17 958	15.1	3	3	153	127
3879	I-II	20 386	16.1	4	2	119	115
Virgo	I-II	1 131	12.5	0	4	556	556
0787	II	40 532	16.9	5	2	98	77
1767	II	21 045	15.7	4	1	158	115
1809	II	23 624	15.8	4	1	128	105
2089	II	21 945	15.8	4	1	111	95
2142	II	26 951	16.0	4	2	149	122
2554	II	31 778	16.9	5	3	252	207
2721	II	34 386	17.0	5	3	274	217
0168	II-III	13 466	15.4	3	2	175	148
0426	II-III	5 486	12.5	0	2	166	146
1020	II-III	19 457	16.0	4	1	149	113
1035	II-III	23 953	15.4	3	2	157	119
1227	II-III	33 577	16.6	5	2	139	103
1367	II-III	6 595	13.5	1	2	166	141
1904	II-III	21 225	15.6	3	2	131	113
1920	II-III	39 273	17.0	5	2	167	126
2255	II-III	24 163	15.3	3	2	229	166
2256	II-III	18 018	15.3	3	2	162	140
1412	III	25 003	15.9	4	2	162	134
2048	III	28 330	16.0	4	1	122	108
2061	III	23 024	15.7	4	1	129	100
2065	III	21 765	15.6	3	2	195	151
2151	III	10 943	13.8	1	2	190	177
2197	III	9 223	13.9	1	1	119	106

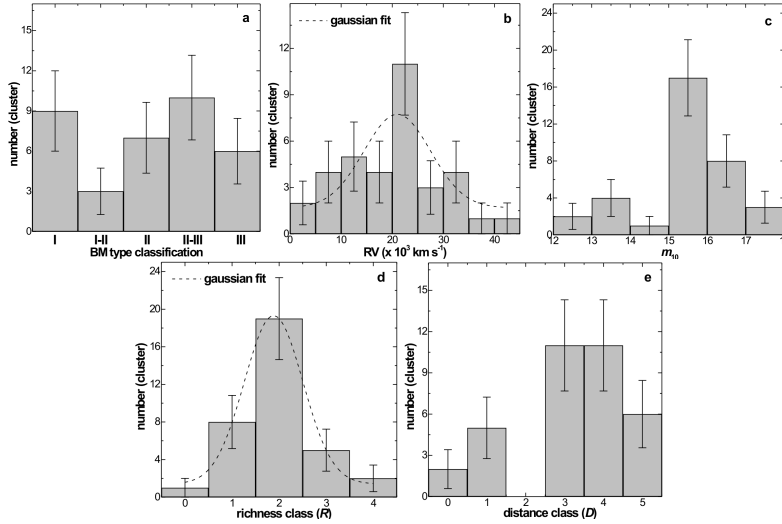


**Figure 2.** The distributions of (a) BM (Bautz & Morgan 1970) type classification, (b) radial velocity  $RV$ , (c) magnitude of the tenth brightest cluster member ( $m_{10}$ ), (d) richness class ( $R$ ) and (e) distance class ( $D$ ) of the clusters studied. The observed values with statistical  $\pm 1\sigma$  error bars are shown. The dashed lines (b,d) represent the gaussian fit.

The estimation of background galaxies in the cluster region was based on the area distribution of background galaxies around the cluster region. It is estimated that the background contamination of galaxies in the investigated cluster region is  $\sim 10 \pm 5\%$ . These objects include more distant lensed galaxies. We removed these galaxies from the database.

The foreground field galaxies in the investigated cluster region were identified with the help of the Uppsala General Catalogue of Galaxies (Nilson 1973, 1974; UGC hereafter), the Third Reference Catalogue of Bright Galaxies (de Vaucouleurs et al. 1991), the ESO/Uppsala Survey of the ESO (B) Atlas (Lauberts 1982), Photometric Atlas of Northern Bright Galaxies (Kodaira et al. 1990) and the Southern Galaxy Catalogue (Corwin et al. 1985). These field galaxies have been removed from the database. The errors in the PAs were determined by comparing the measured values with known values in the catalogue (mainly UGC). It turned out to be less than  $\pm 10^\circ$ . The error in diameters, mainly due to a limited step size, was estimated to be 5 arcsec. For a distant cluster this limit is larger in absolute value than that of the nearby cluster. This may cause a systematic error in the diameter distribution of galaxies in the cluster. However, their effect in the optical search limit is well within the  $1\sigma$  error limit.

We have included all types of clusters in our database. Fig. 2 shows the morphology, mean  $RV$ , magnitude of the tenth brightest cluster member ( $m_{10}$ ), richness ( $R$ ) and distance class ( $D$ ) distribution of the cluster. Our database contain all types of clusters: regular or symmetrical (BM I), intermediate (BM I-II, II, II-III) and irregular or asymmetrical (BM III) (Fig. 2a). The maximum and minimum  $RV$ s of the clusters are  $\sim 1\,000$  (Virgo) to  $\sim 41\,000$  (A0787)  $\text{km s}^{-1}$  (Fig.

2b). There are 11 clusters that have mean  $RV$  20 000 to 25 000  $\text{km s}^{-1}$  in our database. Because of this bin, the centre of the gaussian fit is found at 21 000  $\text{km s}^{-1}$  (Fig. 2b). There are 25 clusters that have  $m_{10}$  value in the range 15 to 17 (Fig. 2c). The centre of the gaussian fit of  $R$  distribution is found at  $\sim 2$  (Fig. 2d). There were 19 clusters that have Abell richness  $R = 2$ . There were no clusters that have  $D = 2$  in our database (Fig. 2e). Eleven each clusters are at the distance class  $D = 3$  and 4.

### 3. Method of analysis

Astronomical data are often accompanied by several selection effects. One can sometimes regard these selection effects as noise in the database. In such situations, even though all control parameters (independent variables) remain constant, the resultant outcomes (dependent variables) vary. A process of quantitatively estimating the trend of the outcomes, also known as regression or curve fitting, therefore becomes necessary. In this work, we have analysed the database of 6 244 galaxies in different context. For this we performed linear and polynomial fits to the diameter ( $a$ ) and position angle (PA) distributions.

In addition to this, we have carried out three statistical tests, namely, chi-square, auto-correlation and Fourier in order to distinguish anisotropy from isotropy in the PA-distribution. We set the chi-square probability  $P(> \chi^2) = 0.050$  as the critical value to discriminate isotropy from anisotropy. We expect an auto correlation coefficient  $C \rightarrow 0$  for an isotropic distribution. For a detailed description of the statistical tests see Godłowski (1994) and Flin & Godłowski (1986). See Appendix for the details of the Fourier test.

## 4. Results

### 4.1 Optical search limit

The distribution of the apparent diameters of the galaxies in the cluster can give information about the completeness of the optical catalogue. Here we consider a ‘toy model’ by assuming a homogeneous distribution of galaxies in space having equal linear diameter  $d_i$ . The spatial density of galaxies  $\rho_i$  is assumed to be constant. The total number of galaxies of diameter  $d_i$  within a given distance  $r$  is given by,

$$N_i(r) = \frac{4}{3}\pi\rho_i r^3 \quad (1)$$

and the angular diameter  $\alpha$  of the galaxies is,

$$\alpha = \frac{d_i}{r}. \quad (2)$$

The total number of galaxies within a given angular diameter  $\alpha$  is given by,

$$N_i(\alpha) = \frac{4}{3}\pi\rho_i d_i^3 \alpha^{-3}. \quad (3)$$

Summing this equation for all linear diameters

$$N(\alpha) = \frac{4}{3}\pi\alpha^{-3} \times \Sigma\rho_i d_i^3 \quad (4)$$

Taking logarithms of both sides,

$$\log(N) = \log\left(\frac{4}{3}\pi\Sigma\rho_i d_i^3\right) + \log(\alpha^{-3}) \quad (5)$$

and defining  $C = \log\left(\frac{4}{3}\pi\Sigma\rho_i d_i^3\right)$ ,

$$\log(N) = C - 3 \times \log(\alpha) \quad (6)$$

Thus, the logarithm of the total number of galaxies having an apparent diameter ( $\alpha$ ) greater or equal to a given limit has a slope of  $-3$ .

We know that the effect of clustering is neglected in this ‘toy model’. Due to this assumption we expect to get large deviations from the  $-3$  slope line in the diameter distribution of cluster galaxies (see Fig. 3). We intend to study whether this deviation shows any systematic dependence on cluster parameter. In the future, we intend to develop a method so that we can define a physical reference system in the cluster itself. Here we do not use Zwicky or de Vaucouleurs profiles for density distribution in the cluster. Neither we use Mattig’s formula. We will address all these profiles in our next work.

Fig. 3 shows  $\log(N)$  versus  $\log(\alpha)$  plots for all 35 clusters. In equation (6), the symbol  $\alpha$  corresponds to the major diameter ( $a$ ) of galaxies. In Fig. 3,  $\log(N)$  and  $\log(\alpha)$  are represented by ‘number’ and ‘major diameter (arcmin)’, respectively. The second column of the Table 3 gives the slope of the best fit line. The optical search limit ( $SL$ ) of the clusters are estimated using ‘ $-3$  slope’ line. The third column of the table 3 lists the values of the search limit ( $SL$ ) up to which the optical catalogue of the clusters is said to be complete.

Fig. 3a shows the distribution of the apparent diameters of galaxies in the cluster Abell 0042. In the figure, the solid and dashed lines represent the  $-3$  slope and the best fit lines, respectively. The slope of the best fit line is found to be  $-2.6$ . The observed diameter distribution is found to deviate from these lines. The point at which the diameter starts to deviate from the solid line ( $-3$  slope line) is taken as the ‘limit’ up to which the optical catalog is assumed to be complete. In this cluster, this limit is found to be 0.6 arcmin. So, the catalog of galaxies in A0042 that have apparent major diameter  $\geq 0.6$  arcmin is complete. In other words, the diameter distribution of 48 galaxies (about 30%) is found to be deviated from our ‘toy model’. This deviation clearly hints the clustering phenomena. The situation is worse in the cluster A0401, where the diameter distribution of 198 galaxies ( $\sim 75\%$ ) is found to be deviated from the  $-3$  slope line (i.e., from our

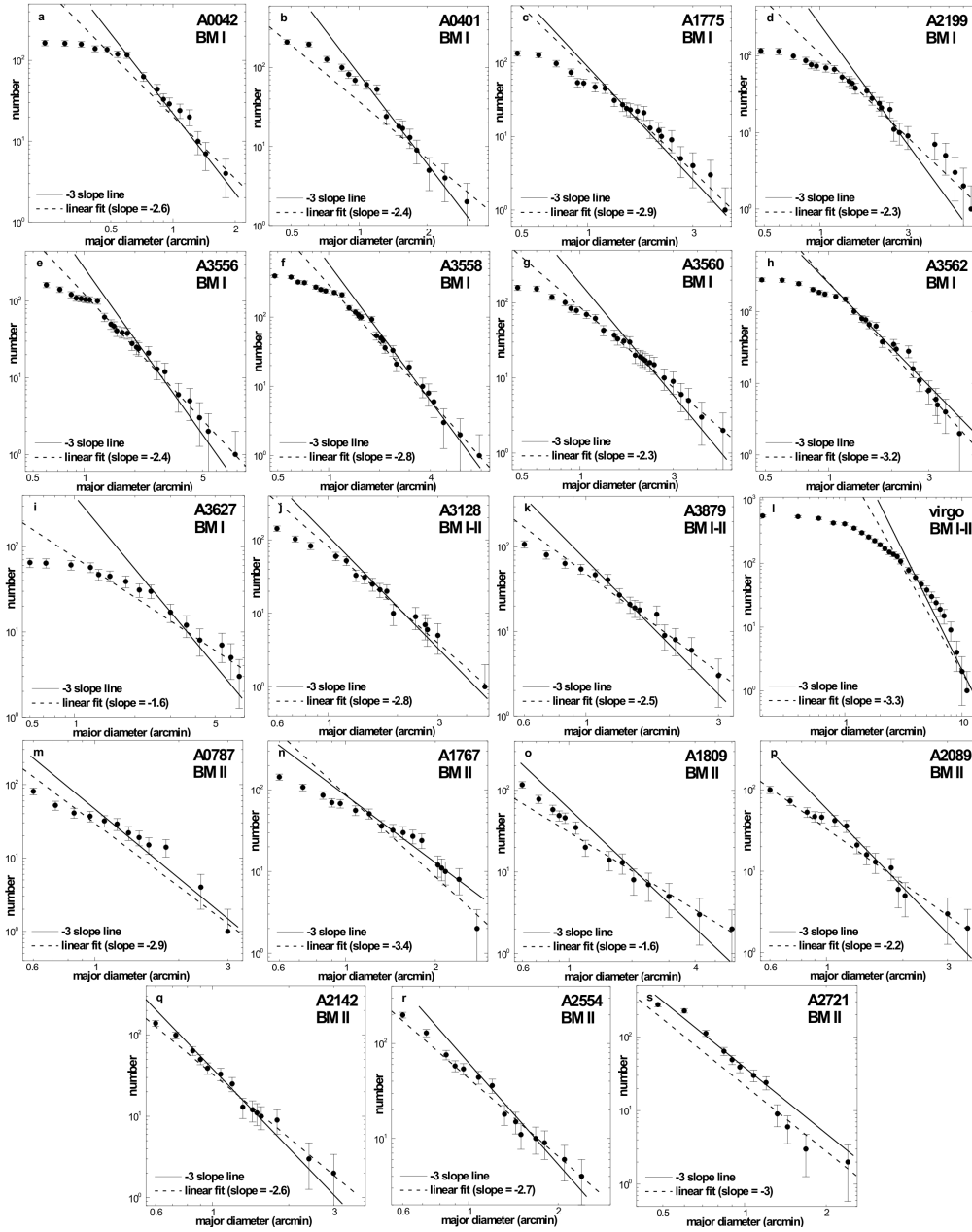


**Figure 3.** The distribution of the major diameter (in arcmin) of galaxies in 35 cluster. The name of the cluster and their morphology (BM type) are given. The axes are in logarithm scale. The solid and dashed lines represent the theoretical line having slope ‘-3’ and the best fit line, respectively. The observed values with  $\pm 1\sigma$  statistical error bars are shown.

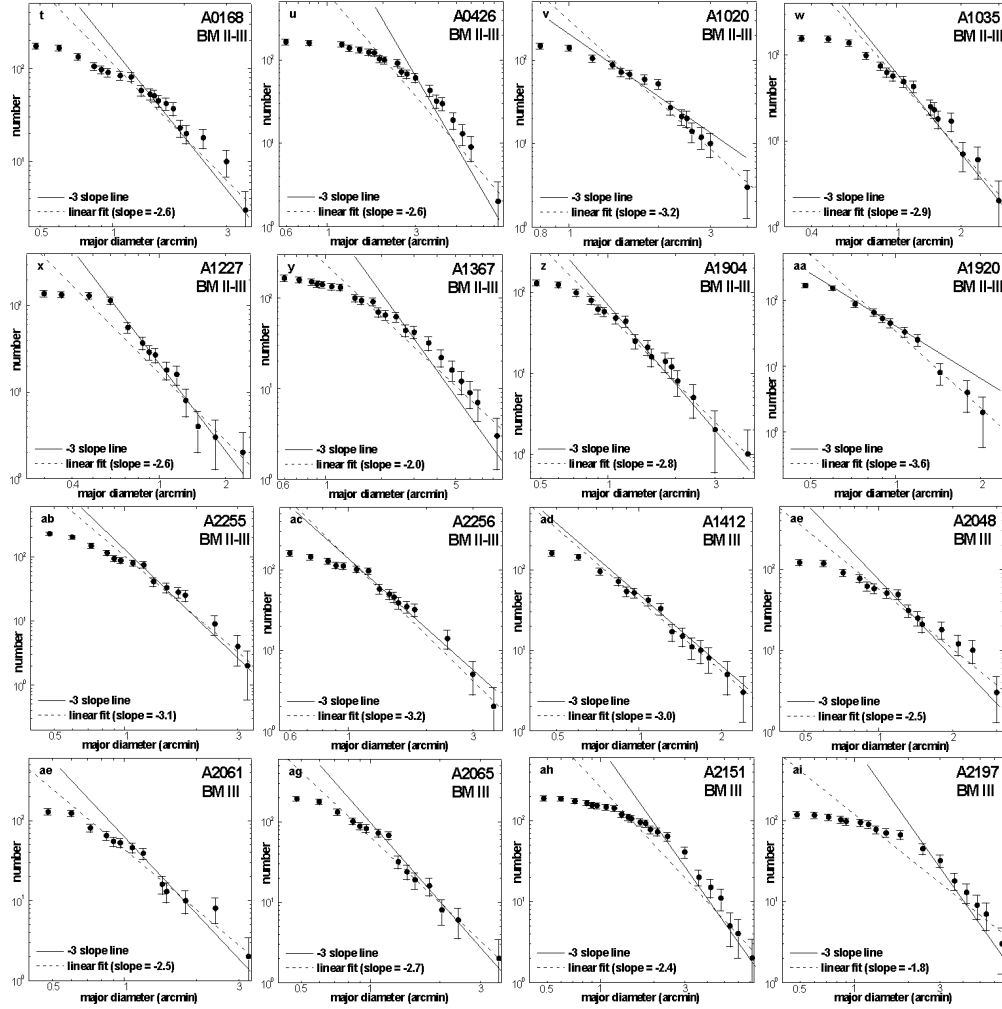


Figure 3. (continued)

‘toy model’). In this cluster the clustering effect is stronger than that of the previous (A0042). We do not bother about this. We intend to see whether the optical search limits in the investigated clusters are random or these show a preference.

The  $SL$  is found to be minimum (0.6 arcmin) for 4 clusters (A0042, A1227, A1920 and A2721). The distance class ( $D$ ) of these cluster is 5. The nearest cluster ( $D = 0$ ), i.e., the Virgo cluster shows maximum  $SL$  value (3.5 arcmin) (Table 3). In this cluster, the diameter distribution of 478 galaxies (about 86%) is found to be deviated from our ‘toy model’. Thus, for the distant cluster, the deviation is smaller than that of the distant cluster. The  $SL$  value of the members of

the Shapley Supercluster A3556, A3558, A3560 and A3562 are found to be 1.8, 1.8, 1.68 and 1.20 arcmin, respectively.

In order to study  $RV$  dependence on optical search limit, we plotted mean  $RV$  of the cluster versus  $SL$  value (Fig. 5a). A good agreement between the linear (solid line) and the second order polynomial fit (dashed line) can be seen. It seems that the  $SL$  value decreases with the increase of the mean  $RV$  of the cluster. The implications of this result is discussed in Sect. 4.3.

## 4.2 Anisotropy in the position angle distribution

In the method of Hawley & Peebles (1975), the observed PAs and axial ratio distributions are analysed independently. They also introduced the Fourier method of analysing PA histograms. Fig. 4 shows the PA-distribution of galaxies in cluster. In the figure,  $PA = 0^\circ$  or  $180^\circ$  corresponds to the galactic rotation axes lying in the equatorial plane.

Here we analyse the distribution of the equatorial PAs of galaxies. The conditions for anisotropy are the following: the chi-square probability  $P(> \chi^2) < 0.050$ , correlation coefficient  $C/\sigma(C) > 1$ , first order Fourier coefficient  $\Delta_{11}/\sigma(\Delta_{11}) > 1.5$ , and the first order Fourier probability  $P(> \Delta_1) < 0.150$ . The last three columns of Table 3 list these statistical parameters. In the Fourier test,  $\Delta_{11}/\sigma(\Delta_{11}) < 1$  (i.e., negative) suggests that the PA of galaxies tend to lie in the equatorial plane. In other words, a negative  $\Delta_{11}$  suggests that the rotation axis of galaxies tend to be oriented perpendicular with respect to the equatorial plane. Similarly,  $\Delta_{11} > 0$  (i.e., positive) indicates that the rotation axis of galaxies tend to lie in the equatorial plane. Figure 4 shows the PA-distribution of galaxies in the investigated cluster. In the histograms, a hump at  $90^\circ \pm 45^\circ$  suggests that the PAs of galaxies tend to lie in the equatorial plane.

All 9 BM type I clusters show isotropy in chi-square test (eighth column, Table 3). The chi-square probability ( $P(> \chi^2)$ ) is found to be  $> 5\%$  in these clusters. In the Fourier test, the cluster A3560 showed negative  $\Delta_{11}$  value at  $> 1.5\sigma$  level, suggesting anisotropy (Table 3). In the histogram (Fig. 4g), a hump at  $90^\circ$  can be seen. This hump lead this cluster to show a preferred alignment in the PA-distribution. Thus, the PA of galaxies in the cluster A3560 tend to lie in the equatorial plane.

The  $\Delta_{11}$  value is found to be positive at  $> 1.5\sigma$  level in all three BM type I-II clusters, suggesting similar preferred alignments in the PA-distribution. The humps at  $170^\circ$  (A3128 & Virgo cluster) and at  $150^\circ$  (A3879) can be seen (Fig. 4j,k,l). Thus, the PA of galaxies in the clusters A3128, A3879 and Virgo tend to be oriented perpendicular to the equatorial plane.

The humps at  $70^\circ$  and  $170^\circ$  lead the cluster A2142 to show a bimodal orientation in the PA-distribution (Fig. 4q). A BM type II cluster (A2089) showed the  $\Delta_{11}$  value  $> 1.5\sigma$ , suggesting anisotropy.

We studied PA-distributions of 10 BM type II-III clusters. A mixed result is found here:  $\Delta_{11}$

**Table 3.** Statistics of optical search limit (second and third columns) and position angle distribution (last six columns). The first column lists the Abell number. The ‘slope’ and ‘SL’ (in arcmin) represent the slope of the best fit line and the optical search limit (see Fig. 3). The last three columns give the chi-square probability ( $P(> \chi^2)$ ), correlation coefficient ( $C/C(\sigma)$ ), first order Fourier coefficient ( $\Delta_{11}/\sigma(\Delta_{11})$ ), and first order Fourier probability  $P(> \Delta_1)$  in the PA-distribution.

Abell	slope	SL	$P(> \chi^2)$	$C/C(\sigma)$	$\Delta_{11}/\sigma(\Delta_{11})$	$P(> \Delta_1)$
0042	-2.6	0.60	0.197	+0.7	-1.2	0.093
0401	-2.4	1.20	0.755	+0.4	+1.2	0.368
1775	-2.9	1.32	0.510	+0.0	+0.9	0.247
2199	-2.3	1.80	0.914	-0.5	-0.5	0.866
3556	-2.4	1.80	0.755	+0.1	-0.3	0.863
3558	-2.8	1.80	0.255	-1.7	-0.2	0.734
3560	-2.3	1.68	0.532	+0.1	-1.7	0.241
3562	-3.2	1.20	0.282	+0.4	+0.1	0.291
3627	-1.6	2.40	0.184	-1.5	+0.7	0.585
3128	-2.8	1.44	0.055	+0.0	+1.9	0.114
3879	-2.5	1.20	0.313	+0.3	+1.9	0.101
Virgo	-3.3	3.50	0.126	-1.7	+1.9	0.165
0787	-2.9	1.08	0.392	+0.0	-0.3	0.574
1767	-3.4	1.20	0.985	+0.0	-0.4	0.913
1809	-1.6	1.20	0.515	-0.6	+0.1	0.961
2089	-2.2	1.08	0.382	-0.7	+1.7	0.198
2142	-2.6	0.84	0.001	-2.4	+0.5	0.578
2554	-2.7	1.08	0.589	+0.2	-1.3	0.269
2721	-3.0	0.60	0.674	-0.9	+1.2	0.488
0168	-2.6	1.44	0.886	-0.5	-0.2	0.901
0426	-2.6	3.00	0.793	-0.4	+0.0	0.555
1020	-3.2	1.40	0.762	+0.3	+1.6	0.252
1035	-2.9	1.08	0.729	-1.1	+0.6	0.819
1227	-2.6	0.60	0.039	-1.0	+0.5	0.690
1367	-2.0	2.40	0.004	-1.3	+0.5	0.264
1904	-2.8	1.08	0.028	+1.4	-2.0	0.137
1920	-3.6	0.60	0.008	+1.7	+1.5	0.001
2255	-3.1	1.20	0.746	+0.7	+2.0	0.124
2256	-3.2	1.08	0.038	+1.2	+1.0	0.441
1412	-3.0	0.84	0.128	-0.3	+1.8	0.104
2048	-2.5	1.08	0.073	-0.1	+0.2	0.970
2061	-2.5	1.08	0.254	-0.9	+2.0	0.120
2065	-2.7	1.08	0.000	-2.3	+2.1	0.109
2151	-2.3	2.10	0.047	-1.3	+1.3	0.341
2197	-1.8	2.40	0.582	+0.3	-1.3	0.214

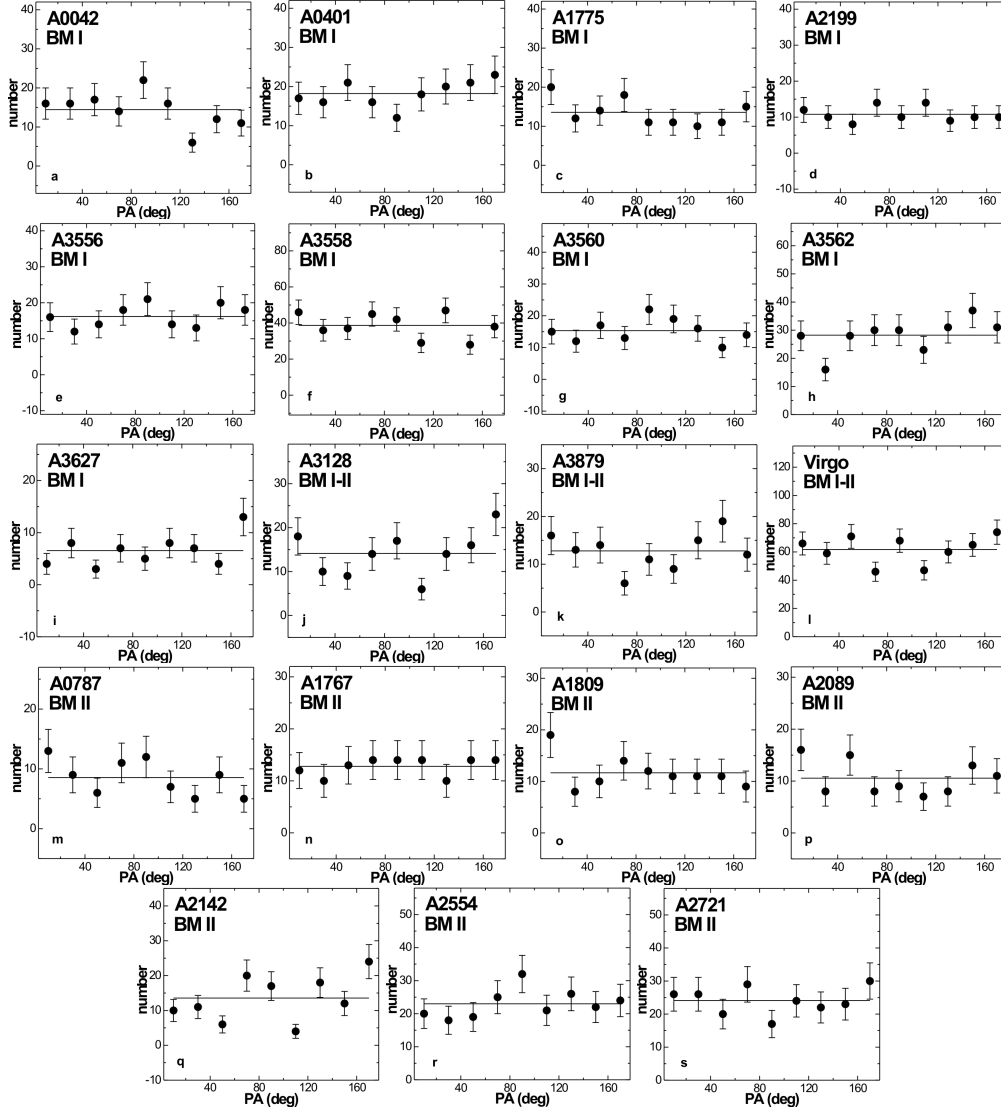


**Figure 4.** Position angle (PA) distribution of galaxies in 35 cluster. The solid circles with statistical  $\pm 1\sigma$  error bars represent the observed PA-distribution. The Abell name and the BM type classifications are given. The solid line represents the expected distribution.

value negative for A1904, positive for A1020, A1920 and A2255. The cluster A1367 showed a bimodal orientation: PA of galaxies tend to be oriented to both the parallel (hump at  $70^\circ$ ) and perpendicular (hump at  $170^\circ$ ) with respect to the equatorial plane (Fig. 4t).

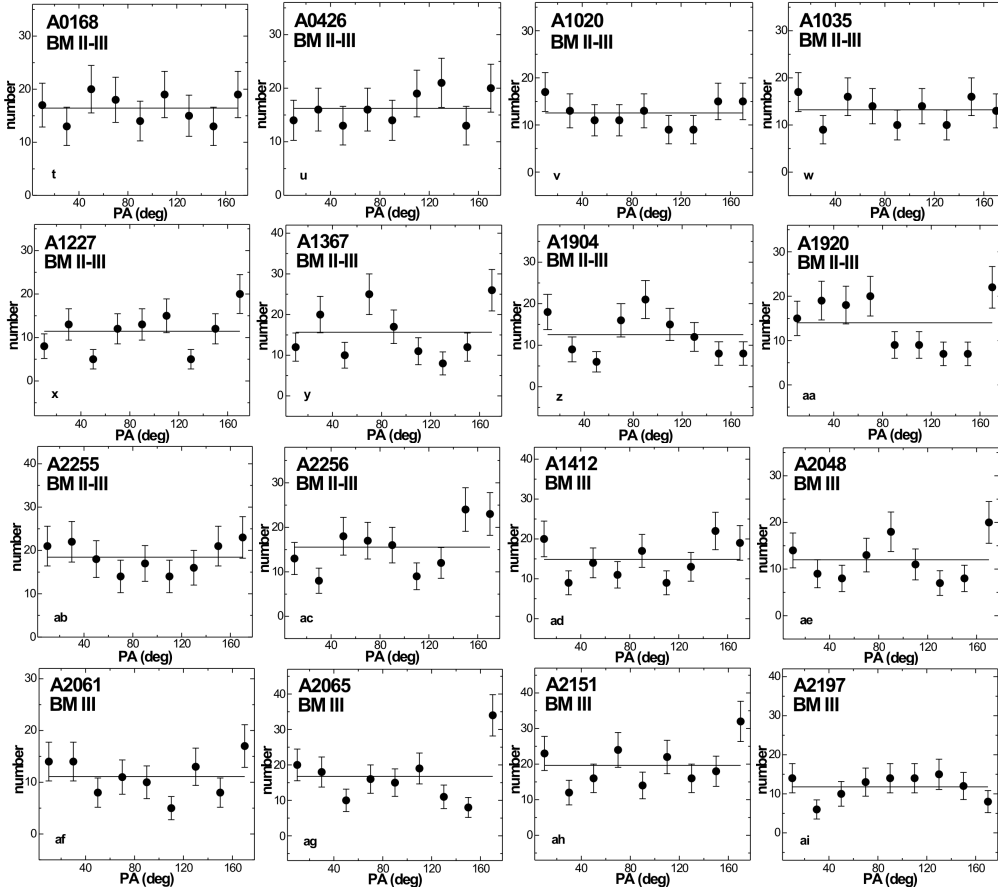
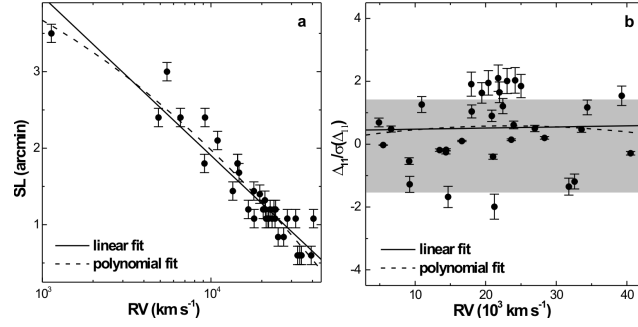


Figure 4. (continued)

Three BM type III clusters (A1412, A2161 & A2065) showed anisotropy in the PA-distribution. The  $\Delta_{11}$  value is found to be positive at  $> 1.5\sigma$  level (Table 3). These clusters showed similar alignments. The PA of galaxies in these clusters tend to be oriented perpendicular to the equatorial plane. The cluster A2048 showed bimodal alignments (Fig. 4ae).

Fig. 5b show the scatter plot between the mean  $R_V$  of the cluster and the orientation parameter ( $\Delta_{11}/\sigma(\Delta_{11})$ ). In the figure, the slope of the linear fit line is approximately null, suggesting no relations between preferred alignments and the mean  $R_V$  of the cluster. A good agreement between the linear and the second order polynomial fit supports this result. Thus, the preferred alignments of galaxies in the clusters are found to be independent of the mean  $R_V$  of the cluster.



**Figure 5.** The RV versus (a) optical search limit ( $SL$ ) and (b) orientation parameter ( $\Delta_{11}/\sigma(\Delta_{11})$ ) in the PA distribution of galaxies in 35 Abell cluster. Solid circle with error bars represent a cluster. The solid and dashed lines correspond to the linear and polynomial (second order) fits, respectively. The isotropy and anisotropy is separated by the grey-shaded region:  $-1 \leq \Delta_{11}/\sigma(\Delta_{11}) \leq +1$  for the isotropy and  $\Delta_{11}/\sigma(\Delta_{11}) > \pm 1.5$  for anisotropy. In between  $1\sigma$  and  $1.5\sigma$  we consider weak anisotropy.

### 4.3 Discussion

Here we discuss possible relationship between the mean  $RV$  of the cluster and the optical search limit ( $SL$ ) and position angle (PA) of galaxies in the cluster.

We suspect a relation between the optical search limit ( $SL$ ) and the mean  $RV$  of the cluster (Fig. 5a). A good agreement between the linear (solid line) and the second order polynomial fit (dashed line) are found. The equation of the linear fit is  $\log(SL) = -2.1 \times \log RV + 10.2$ . The slope of the linear fit are found to be negative  $\sim 2.0$ , suggesting inverse square law ( $SL \propto 1/RV^2$ ). Thus, the optical  $SL$  decreases with the mean  $RV$  of the clusters. We intend to discuss the effect of this toy model in the Mattig's formula in the future. It is interesting that, up to a certain limit, diameter distribution of large scale structures obey inverse square law with their radial velocities. The deviation in the diameter distribution clearly hints the clustering phenomena: the larger the deviation the denser the clustering.

No relation between the mean  $RV$  of the cluster and the orientation parameter ( $\Delta_{11}/\sigma(\Delta_{11})$ ) is noticed in the PA-distribution. The slope of the best fit line is found to be parallel (approximately) to the X-axis, suggesting random alignments (Fig. 5b). Thus, the preferred alignments of galaxies in the clusters are found to be independent of the mean  $RV$  of the cluster.

The preferred PA of galaxies in the cluster and the cluster morphology (BM type) is found to be independent. As expected, no dependence is observed between the cluster morphology and the optical search limit.

Thus, the value of the optical search limit depends upon the mean  $RV$  of the cluster. However, the preferred PA is found to be independent of the mean  $RV$  of the cluster.

#### 4.4 Previous works

The PA-distribution of 126 galaxies in Abell 2199 was studied by Thompson (1976). The chi-square probability  $P(> \chi^2)$  was 48% in his calculation suggesting no significant alignment. Our result is similar to that result obtained by Thompson (1976) in the PA-distribution. We found 91% probability in the chi-square test (Table 3). The only cluster in which Thompson (1976) found a significant preference in the PA-distribution was Abell 2197. He analysed the PA-distribution of 114 galaxies in Abell 2197 and found anisotropy whereas Adams et al. (1980) analysed 58 galaxies of the same cluster and found isotropy. We found isotropy ( $P(> \chi^2) = 58\%$ ) when analysing PA-distribution of 106 galaxies in this cluster. So, our results agree with Adams et al. (1980) in the PA-distribution. Thompson (1976) found isotropy when analysing PA-distribution of 115 galaxies in Abell 2151. Our result does not agree with Thompson's result. We found anisotropy when analysing PA-distributions of 177 galaxies in this cluster. This disagreement might be due to the rich (50% more) database.

The core of the Shapley concentration is dynamically very active; the main cluster Abell 3558 appears to be interacting with the other clusters Abell 3562 and Abell 3556 (Bardelli et al. 1994). In our study, the galaxies in the main cluster Abell 3558 show isotropy whereas Abell 3560 shows anisotropy in the Fourier test ( $\Delta_{11}/\sigma(\Delta_{11}) = -1.7$ ). In a substructure analysis Bardelli et al. (1998) briefly discussed the core of the Shapley concentration and suggested that the core complex is the result of a series of incoherent group-group and cluster-group mergings.

Oegerle & Hill (2001) performed a dynamical study of 25 clusters containing a centrally located cD galaxy. These are BM type I clusters. The shape of the cluster velocity distribution is found gaussian for A1767 and A1809 whereas non-gaussian for A2089. Interestingly, we found anisotropy for A2089 and isotropy for A1767 and A1809 in the PA-distribution. Thus, the clusters that have non-gaussian type velocity distribution show anisotropy in PA-distribution of their galaxies. Oegerle & Hill (1994) studied dynamics of A1809 using redshift data reported by Hill & Oegerle (1993). The cD galaxy of this cluster shows no significant peculiar velocity with respect to the global velocity distribution. We do not notice preferred alignments in this cluster. Hence, this cluster behaves as a late-type cluster (like BM III). Probably, the BM type classification misleads this cluster.

The cluster A2142 is a cooling core cluster containing active radio galaxies in the core (Markovic et al. 2004). The radio sources in this cluster might play an important role in the energetics of the cooling cluster core. We noticed a bimodal orientation in the PA-distribution of galaxies in A2142 cluster: the galactic planes of galaxies tend to orient both the parallel and perpendicular with respect to the equatorial plane. This alignment might have a connection with energetics of the cluster core.

Gołowski et al. (2010) studied the spatial orientations of galaxies in the 247 optically selected rich Abell clusters with respect to the Supergalactic coordinate system. Four clusters (A0042, A2554, A2721 & A3128) are common with the present work. We found no preferred alignments in the equatorial PA distribution when analysing 130 galaxies in the cluster A0042.

Godłowski et al. (2010) studied 76 galaxies having axial ratios ( $b/a$ ) less than 0.75 in the cluster A0042 and found a preferred alignments. They noticed that the galactic planes of galaxies in A0042 tend to lie in the Supergalactic plane, i.e., Local Supercluster. Our results support Godłowski et al. (2010) conclusion that the values of statistics increase with the increase of the member galaxies in the cluster. They found no preferred alignments of Supergalactic PA distribution of galaxies in the clusters A2254, A2721 and A3128. We noticed a preferred alignment in the equatorial PA distribution of galaxies in A3128. Godłowski et al. (2010) noticed a weak dependence between the preferred alignments and Bautz - Morgan type cluster morphology. Aryal, Paudel & Saurer (2007) noticed a weak dependence with morphology: a systematic change in the galaxy alignments from early-type (BM I) to late-type (BM III) clusters while studying a database of 25 Abell clusters.

No authors have estimated the optical search limit of the clusters studied.

## 5. Conclusion

We measured diameters and the position angles of 6 244 galaxies in POSSII and ESO films using 25-fold magnification microscope. These galaxies belongs to the 34 Abell cluster that have mean  $RV \sim 1\,000$  to  $43\,000$  km s<sup>-1</sup>. We estimated the optical search limit for the major diameters of the galaxies in the clusters and studied their relation with the mean velocity of the cluster. The equatorial position angle distributions of galaxies in the clusters are studied. The expected distributions are compared with observed distributions using three statistical tests: chi-square, auto-correlation and the Fourier. Our results are as follows:

- The minimum value of the optical search limit ( $SL$ ) is found to be 0.6 arcmin for 4 clusters (A0042, A1227, A1920 and A2721). These are distant ( $D = 5$ ) cluster. As expected, the Virgo cluster (nearest cluster,  $D = 0$ ) showed maximum  $SL$  value (3.5 arcmin). Thus, the  $SL$  value of the cluster is found to decrease with the mean  $RV$  of the cluster. We propose an empirical relation, i.e.,  $SL \propto 1/RV^2$ .
- The alignments of galaxies in the cluster is found to be independent of the mean  $RV$  of the cluster. In few clusters (A3560, A3128, A3879, A2089, A1020, A1904, A2255, A1412, A2061, A2065 and the Virgo) we noticed preferred alignments.
- The preferred alignments of galaxies in the cluster and the cluster morphology is found to be independent. As expected, no relation is observed between the cluster morphology and the optical search limit.

Thus, the optical search limit depends upon the mean  $RV$  of the cluster whereas the preferred PA is found to be independent of the mean  $RV$  of the cluster. In the future, we intend to address the optical search limit in a better way and focus our work on the role of the dark matter in the visible mass distribution mechanism within the cluster.

## Acknowledgments

The authors wish to thank the referee for insightful comments. B. Aryal is grateful to the University of Innsbruck as well as to its Institute of Astro- and Particle Physics for financial support for a research stay during October to December 2009. We are indebted to Prof. Qaisar Shafi, Department of Physics & Astronomy, University of Delaware, USA for his comments and suggestion during 2009 BCVSPIN School, Beijing. We acknowledge Mr. Bhim Chamlagain and Mr. Prakash Thapa for their help during data reduction. This research has made use of the POSS II and ESO prints available at University of Innsbruck, Austria and, NASA/IPAC Extragalactic Database (NED) which is operated by the Jet Propulsion Laboratory, California Institute of Technology, under contract with the National Aeronautics and Space Administration.

## References

- Abell G.O., Corwin H.G., Olowin R.P., 1989, *ApJS*, 70, 1 (ACO)
- Adams M.T., Strom K.M., Strom S.E., 1980, *ApJ*, 238, 445
- Argyres P.C., Groth E.J., Peebles P.J.E., Struble M.F., 1986, *AJ*, 91, 471
- Aryal B., Saurer W., 2004, *A&A*, 425, 871
- Aryal B., Saurer W., 2005, *A&A*, 432, 841
- Aryal B., Saurer W., 2006, *MNRAS*, 366, 438
- Aryal B., Paudel S., Saurer W., 2007, *MNRAS*, 379, 1011
- Bardelli S., Zucca E., Vettolani G., Zamorani G., Scaramella R., Collins C. A., MacGillivray H. T., 1994, *MNRAS*, 267, 665
- Bardelli S., Pisani A., Ramella M., Zucca E., Zamoreni G., 1998, *MNRAS*, 300, 589
- Barkan R., Loeb A., 2003, *Nature*, 421, 341
- Bautz L.P., Morgan W.W., 1970, *ApJ*, 162, L149
- Binggeli B., Sandage A., Tammann G.A., 1985, *AJ*, 90, 1681
- Corwin H.G., de Vaucouleurs A., de Vaucouleurs G., 1985, *Univ. Texas Monogr. Astron.*, 4, 1
- de Vaucouleurs, G., de Vaucouleurs A., Corwin et al., 1991, *Third Reference Catalogue of Bright Galaxies*, Springer-Verlag, New York
- Djorgovski S., 1983, *ApJ*, 274, L7
- Flin P., Godłowski W., 1986, *MNRAS*, 222, 525
- Godłowski W., 1994, *MNRAS*, 271, 19
- Godłowski W., Piwowarska P., Panko E., Flin P., 2010, *ApJ*, 723, 985
- Godwin J., Metcalfe N., Peach J., 1983, *MNRAS*, 202, 113
- Gregory S., Thompson L., Tift W., 1981, *ApJ*, 243, 411
- Hawley D.L., Peebles P.J.E. 1975, *AJ*, 80, 477
- Hill J.M., Oegerle W.R., 1993, *AJ*, 106, 831
- Kodaira K., Okamura S., Ichikawa S., 1990, *Photometric Atlas of Northern Bright Galaxies*, Univ. of Tokyo Press, Tokyo
- Lauberts A., 1982, *ESO/Uppsala Survey of the ESO B Atlas*, ESO, Garching bei Muenchen
- MacGillivray H.T., Dodd R.J., 1979a, *MNRAS*, 186, 69
- MacGillivray H.T., Dodd R.J., 1979b, *MNRAS*, 186, 743
- MacGillivray H.T., Dodd R.J., 1985, *A&A*, 145, 269
- Markovic T., Owen F.N., Eilek J.A., 2004: in Reiprich T.H., Kempner J.C., Soker N., eds., *Proc. The Riddle of Cooling Flows in Galaxies and Clusters of Galaxies E28*, Virginia, p.61

- Nilson P., 1973, Uppsala General Catalogue of Galaxies, Nova Acta Uppsala University, Ser. V:A, Vol.1  
 Nilson P., 1974, Upps. Astron. Obs. Rep., 5  
 Oegerle W.R., Hill J.M., 1994, AJ., 107, 857  
 Oegerle W.R., Hill J.M., 2001, AJ., 122, 2858  
 Peebles P.J.E., 1988, ApJ., 332, 17  
 Strom S., Strom K., 1978, AJ., 83, 732  
 Thompson L.A., 1976, ApJ., 209, 22  
 Tully R.B., 1988, Nearby Galaxy Catalog. Cambridge Univ. press, Cambridge

## Appendix A

### Fourier Test

The Fourier test is useful when the deviation from isotropy is slowly varying with the angles (in our case, PA). In the PA-distribution, Fourier test gives the clue regarding the deviation from isotropy. Taking first order Fourier mode, the Fourier series is given by

$$N_k = N_{0k}(1 + \Delta_{11} \cos 2\beta_k + \Delta_{21} \sin 2\beta_k + \dots). \quad (7)$$

Here  $N$  denotes the total number of solutions for galaxies in the sample,  $N_k$  the number of solutions in the  $k^{\text{th}}$  bin,  $N_{0k}$  the mean number of solutions per bin,  $N_{0k}$  the expected number of solutions in the  $k^{\text{th}}$  bin, and the angle  $\beta_k$  represents the PA in the  $k^{\text{th}}$  bin. The Fourier coefficients  $\Delta_{11}$  and  $\Delta_{21}$  are the parameters of the distributions. We obtain the following expressions for the Fourier coefficients  $\Delta_{11}$  and  $\Delta_{21}$ ,

$$\Delta_{11} = \sum (N_k - N_{0k}) \cos 2\beta_k / \sum N_{0k} \cos^2 2\beta_k \quad (8)$$

$$\Delta_{21} = \sum (N_k - N_{0k}) \sin 2\beta_k / \sum N_{0k} \sin^2 2\beta_k. \quad (9)$$

The standard deviations ( $\sigma(\Delta_{11})$ ) and ( $\sigma(\Delta_{21})$ ) can be estimated using the expressions,

$$\sigma(\Delta_{11}) = (\sum N_{0k} \cos^2 2\beta_k)^{-1/2} \quad (10)$$

$$\sigma(\Delta_{21}) = (\sum N_{0k} \sin^2 2\beta_k)^{-1/2}. \quad (11)$$

The probability that the amplitude

$$\Delta_1 = (\Delta_{11}^2 + \Delta_{21}^2)^{1/2} \quad (12)$$

is greater than a certain chosen value is given by the formula

$$P(> \Delta_1) = \exp(-nN_0\Delta_1^2/4) \quad (13)$$

with standard deviation

$$\sigma(\Delta_1) = (2/nN_0)^{1/2}. \quad (14)$$

The Fourier coefficient  $\Delta_{11}$  gives the direction of departure from isotropy. The first order Fourier probability function  $P(>\Delta_1)$  estimates whether (smaller value of  $P(>\Delta_1)$  or not (higher value of  $P(>\Delta_1)$ ) a pronounced preferred orientation occurs in the sample. The positive (negative)  $\Delta_{11}$  value at  $> 1\sigma$  level suggests that the PAs of the galaxies tend to be oriented perpendicular (parallel) to the equatorial plane.